Journal of Catalysis **210,** 229–236 (2002)
doi:10.1006/jcat.2002.3679

Dynamic Behavior of the Surface Structure of Cu/ZnO/SiO_2 Catalysts

W. P. A. Jansen,* J. Beckers,† J. C. v. d. Heuvel,† A. W. Denier v. d. Gon,* A. Bliek,† and H. H. Brongersma*,[1]

*Schuit Institute for Catalysis and Department of Applied Physics, Eindhoven University of Technology, P.O. Box 513, 5600 MB Eindhoven, The Netherlands; and †Department of Chemical Engineering, University of Amsterdam, Nieuwe Achtergracht 166, 1018 WV Amsterdam, The Netherlands

Received March 11, 2002; revised May 8, 2002; accepted May 8, 2002

In order to grasp the dynamic behavior of the surface composition of Cu/ZnO-based catalysts, the surface atomic densities of ^{63}Cu and ^{68}ZnO were determined separately with static LEIS on ^{63}Cu/^{68}ZnO/SiO_2 catalysts. Our data show that the methanol synthesis activity and surface composition of ^{63}Cu/^{68}ZnO/SiO_2 depend strongly on the reduction temperature between 473 and 673 K. The catalyst surface is strongly enriched in ZnO under methanol synthesis conditions. The oxidation state of the Cu species in the outermost atomic layer of the Cu/ZnO/SiO_2 surface has been determined by performing LEIS in combination with adsorptive decomposition of N_2O. The observed oxidation behavior of the Cu species differs clearly from pure metallic Cu. This oxidation behavior and the methanol synthesis activity of the reduced catalyst surface are explained in terms of the formation of Cu(I)/ZnO with oxygen vacancies and are shown to be clearly affected by the reducing agent (being 5% CO/5% CO_2/90% H_2 or pure H_2). © 2002 Elsevier Science (USA)

Key Words: **methanol synthesis; Cu/ZnO catalysts; Cu/ZnO/SiO_2 catalysts; LEIS; ISS; adsorptive N_2O decomposition; surface characterization; surface oxidation state.**

1. INTRODUCTION

Cu/ZnO-based catalysts are commercially applied in many industrial processes, such as the production of methanol from synthesis gas, the low-temperature shift reaction, and the synthesis of fatty alcohols from methyl esters. The annual worldwide methanol production alone amounts to 29×10^6 tons (1); hence, the optimization and understanding of these catalysts is of great interest. Although extensive studies have been carried out for more than two decades, controversies remain concerning the nature of the active site in methanol synthesis and the role of ZnO. Surface structures such as Cu on top of ZnO (2–4), Cu(I)/ZnO (5, 6), ZnO on top of Cu (7, 8), mixed Cu–O–Zn (9), and Cu–Zn alloys (10–12) have been proposed for the Cu/ZnO-based catalysts.

Part of the controversy may originate from the frequently reported dynamic behavior of the Cu/ZnO system (see, e.g., 3, 10, 13). It has been speculated that under reaction conditions, part of the ZnO in the catalyst may be reduced and may segregate to the surface (12). Spencer showed that the formation of an α-brass is thermodynamically favored under reaction conditions (14–16). This author also suggests that the presence of traces of CO_2 could significantly change the surface concentration of zinc, which could explain part of the experimental discrepancies (16). To probe the assumed segregation processes, selective information on the *outermost atomic* layer is essential to avoid averaging of the surface and subsurface compositions.

A commonly used method to determine the Cu metal surface area in Cu/ZnO catalysts is by adsorptive decomposition of nitrous oxide (17), according to the reaction

$$2Cu_s + N_2O \rightarrow (Cu_s)_2O + N_2, \qquad [1]$$

where Cu_s denotes a Cu surface site. In spite of its common use, this method entails a fundamental problem: selecting experimental conditions that lead to complete monolayer coverage of Cu with oxygen while excluding subsurface oxidation of Cu. Moreover, the removal by N_2O of oxygen vacancies that are possibly present in ZnO would lead to an overestimation of the Cu metal area when using adsorptive decomposition of nitrous oxide. When Cu–Zn alloys (brasses) are formed, this method is no longer suited to characterizing the Cu surface area and these surfaces may be overestimated by as much as 100% (18).

We have applied low-energy ion scattering (LEIS) to determine the Cu(O) and Zn(O) surface atom densities in the outermost layer. Since the natural Cu and Zn isotopes have similar masses, a separate analysis of Cu and Zn is hampered. Previously we showed that isotopic enrichment allows the separate detection of ^{63}Cu and ^{68}Zn in ^{63}Cu/^{68}ZnO catalysts with LEIS (19). At that time the LEIS measurements revealed a considerable amount of Pb on the surface of the unsupported ^{63}Cu/^{68}ZnO catalyst, originating from the ^{68}ZnO raw material and segregating to the surface during catalyst reduction. In contrast, no impurities were detected on the surface of a ^{63}Cu/^{68}ZnO/SiO_2 catalyst. This seemingly contradictory behavior was attributed to the higher dispersion of Cu and Zn in the ^{63}Cu/^{68}ZnO/SiO_2

[1] To whom correspondence should be addressed. Fax: +31 40 2453587. E-mail: H.H.Brongersma@tue.nl.

0021-9517/02 $35.00

catalyst, or interaction of Pb with the support leading to Pb glasses. As no Pb was detected on the surface of $^{63}Cu/^{68}ZnO/SiO_2$ catalysts, these were used in the present study to investigate the dynamic behavior of the Cu/ZnO system, following reductive treatments in various gas mixtures and at various temperatures.

In principle, LEIS merely provides information on the atomic composition, and not on the oxidation state. The LEIS yield of a pure metal, however, is typically two to five times higher than that of the corresponding metal oxide, due to shielding of the metal by oxygen. Using this difference, information can be obtained on the oxidation behavior/state of the Cu surface species from LEIS measurements before and after N_2O decomposition. This novel method of combining N_2O decomposition and LEIS has two advantages. First, the oxidation state of the Cu can be determined separately from that of the Zn. Second, LEIS assures selective information on the outermost atomic layer. Hence, the oxidation behavior of the Cu surface species and the reliability of adsorptive decomposition of N_2O in assessing the Cu surface area on Cu/ZnO catalysts may be determined.

2. EXPERIMENTAL

2.1. Catalyst Preparation

The synthesis procedure of the isotopically enriched $^{63}Cu/^{68}ZnO/SiO_2$ catalysts was the same as that described in our previous study (19). Isotopically enriched [^{63}Cu]–Cu was obtained from Campro Scientific with a chemical and isotopical purity of >99.875 and >99.87 wt%, respectively. Isotopically pure ^{68}ZnO was obtained from Alfred Hempel GmbH and was chemically and isotopically >98.8 wt% pure. Both Cu and ZnO were converted into their nitrate forms by dissolution in 65% nitric acid (Acros Chimica, p.a.).

A $^{63}Cu/^{68}ZnO/SiO_2$ (12.5 ± 0.4 wt% Cu, 5.15 ± 0.15 wt% Zn; as determined by inductively coupled plasma–atomic emission spectroscopy, 95% confidence interval) catalyst was prepared by homogeneous precipitation as described elsewhere (20). Subsequently, the precipitation mixture was aged for 140 min, after which it was filtered and flushed with demineralized water. The catalyst was dried overnight in air at 363 K.

The dried catalyst samples were pressed (at 250 MPa) into cavities (∅, 2 mm) in alumina disks (∅, 9.9 mm). We have determined that pressing up to at least 2000 MPa does not influence the surface composition of a silica-supported catalyst. Each disk contains two cavities, hence, two identically prepared catalysts. The catalyst was calcined in a flow of 2 $cm^3\ s^{-1}$ of dry air at a temperature of 750 K for 12 h. Subsequently, the catalyst was reduced for 1 h at either 473, 573, or 673 K in a flow of 2 $cm^3\ s^{-1}$ hydrogen (Praxair, 99.999% pure). The heating rate in all cases was 72 $K \cdot h^{-1}$. The reduction procedures correspond to those described elsewhere (3, 13, 20, 21, and references therein), where remarkable changes in catalyst activities for acetone hydrogenation, ester hydrogenolysis, and methanol synthesis are reported, depending on the temperature of the reductive pretreatment. The resulting activated catalysts have been extensively discussed in the cited references. Before transferring the samples to the LEIS setup, these were passivated at 363 K in a flow of 2 $cm^3\ s^{-1}$ 1% N_2O/99% Ar.

In the LEIS setup, the catalysts were rereduced in a pretreatment chamber at the previously applied reduction temperature, either in 5% CO/5% CO_2/90% H_2 or in pure hydrogen at atmospheric pressure for 15 min. In order to prevent subsequent changes in the surface composition, samples were always cooled below 373 K in the reactant mixtures before evacuation was started. Both *in situ* measurements (7) and kinetically calculated time scales (15) show that in this way changes in the surface composition may successfully be prevented. N_2O decomposition was carried out in the LEIS pretreatment chamber for 45 min at 363 K in 5% N_2O/95% He at atmospheric pressure.

The pure ^{63}Cu sample did not receive *ex situ* reduction or calcination and was only reduced in the LEIS pretreatment chamber (30 min in 1 atm H_2 at 573 K). To investigate the shielding of Cu by oxygen atoms for 4 keV Ne^+ scattering, N_2O decomposition was carried out on a sputter-cleaned ^{63}Cu sample in the LEIS pretreatment chamber (45 min in 1 atm 5% N_2O/95% He at 363 K). A pure ^{68}ZnO sample was analyzed after calcination (30 min in 1 atm O_2 at 573 K) and after a subsequent reduction (15 min in 1 atm H_2 at 573 K).

2.2. LEIS

The LEIS experiments were carried out using the ERISS LEIS setup. In this setup a beam of monoenergetic noble gas ions (He^+ or Ne^+ with energies of 3 and 4 keV, respectively) is directed perpendicularly onto the target. The energy distribution of the backscattered ions is analyzed for a fixed scattering angle (145°) with a double toroidal electrostatic analyzer. The analysis is similar to that of the EARISS setup, which has been described in more detail elsewhere (22, 23). This analyzer makes very efficient use of the backscattered ions by measuring simultaneously a considerable part of the energy spectrum contained in 320° of the azimuthal angle. Using this type of analyzer measurements can be carried out using only 10^{13} ions/cm^2. For metallic Cu the 4 keV Ne^+ sputter yield is 3 atoms/ion (24). When the same yield is assumed for ZnO and the number of atoms in the surface of the catalyst amounts to 1.3×10^{15} at/cm^2 (average of Cu (19) and ZnO (25)), a dose of 0.4×10^{15} Ne^+/cm^2 corresponds to the removal of one atomic layer. The 3-keV He^+ sputter yield is 0.25 atoms/ion (24), resulting in a dose of 5.2×10^{15} He^+/cm^2 for the removal of one atomic layer. Hence, the ERISS allows us to perform static LEIS, i.e., with negligible damage. Note that

during the previous study, using the NODUS setup (19), $\sim 10^2$ higher doses had to be used. In the present study both low doses ($\sim 10^{13}$ ions/cm^2) and higher doses ($\sim 10^{15}$ ions/cm^2) were applied, the latter to obtain depth profiles. Depth profiles of the atomic compositions of the different catalysts were obtained by fitting the areas of the Cu and Zn peaks in the ^{63}Cu/^{68}ZnO/SiO$_2$ LEIS spectra to reference spectra measured on pure ^{63}Cu, ^{63}CuO, and ^{68}ZnO as a function of the applied dose. The depth profiles were fitted by assuming the surface consisted of a combination of uncovered CuO and ZnO, as well as CuO and ZnO that were shielded either by hydrogen or by each other. The sputter rates of H, CuO, and ZnO were kept constant in all fits.

2.3. Surface Oxidation State Evaluated with LEIS and Adsorptive N_2O Decomposition

In principle, LEIS provides only information on the atomic densities of the atoms present in the surface, and not on their oxidation state. One cannot tell whether the detected oxygen atoms belong to copper or to zinc oxide. However, in oxides the oxygen atoms (partly) shield the metal atom. Therefore, the experimentally determined 4-keV Ne^+ Cu LEIS yield of a metallic Cu reference sample is a factor of 5 higher than that of oxidized copper formed after exposing the Cu metal to N_2O (30-min treatment in 1 atm 5% N_2O/95% He at 363 K). Similarly, the 4-keV Ne^+ LEIS yield of Zn is a factor of 3.7 higher than that of ZnO. Hence, a comparison of the Cu and Zn LEIS yields of a ^{63}Cu/^{68}ZnO/SiO$_2$ catalyst before and after exposure to N_2O, may provide details of the oxidation state of the surface Cu and Zn atoms. Aluminum disks, containing two catalyst samples each, were analyzed with LEIS before and after exposing them to N_2O. In this way two further identically prepared and pretreated catalysts could be compared to obtain information on the oxidation state of the surface species.

3. RESULTS

3.1. Oxidation State of the Cu and Zn in the Cu/ZnO/SiO$_2$ Catalyst

It is crucial to assess the oxidation state of the copper and zinc atoms in the Cu/ZnO/SiO$_2$ catalyst in order to comprehend the structure–activity relation. As explained before, the combination of LEIS measurements before and after N_2O chemisorption may be used to address this issue. Figure 1 shows the Cu and Zn LEIS signals of reduced ^{63}Cu/^{68}ZnO/SiO$_2$ (hydrogen at 473 K) before (open markers) and after (solid markers) subsequent exposure to N_2O. The figure shows that both the Cu and the Zn LEIS yields did not change significantly (i.e., less than 4%). The Cu and Zn LEIS yields of ^{63}Cu/^{68}ZnO/SiO$_2$ reduced in hydrogen at 673 K decreased about 20% on N_2O decomposition. Hence, the oxidation behavior of Cu and Zn species in the surface

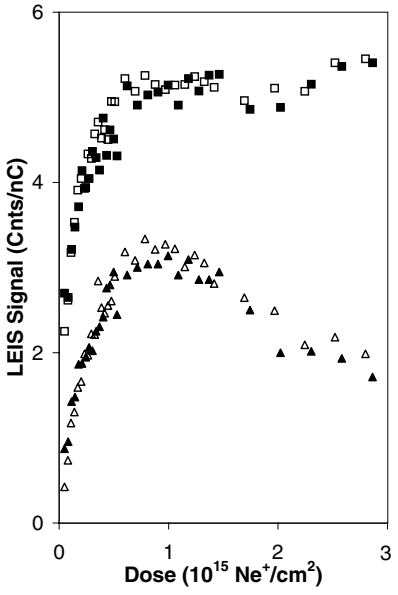

FIG. 1. The Zn (triangles) and Cu (squares) atomic density of Cu/ZnO/SiO$_2$ as a function of a 4-keV Ne^+ dose. The solid data points were obtained after reduction at 473 K in pure H_2; the open data points were obtained after the sample was subsequently exposed to N_2O at 363 K.

of a reduced ^{63}Cu/^{68}ZnO/SiO$_2$ catalyst is different from that of pure, metallic Cu and Zn, where N_2O exposure results in a reduction of the LEIS signal with a factor of 3.7–5. One may therefore conclude that less than 5% (after reduction at 473 K) or 25% (after reduction at 673 K) of both the Cu and Zn species at the surface is metallic. The fact that N_2O decomposition has only a minor impact on the LEIS yields of reduced ^{63}Cu/^{68}ZnO/SiO$_2$ can only be explained by the presence of (partly) oxidized Cu and Zn that may well be present in the form of Cu(I)/ZnO (5, 6). The presence of oxygen vacancies (26) may explain the observed 20% decrease in the Cu and the Zn signal after the N_2O treatment of those catalysts that were previously reduced at 673 K. We have used pure CuO and ZnO to calibrate surface area percentages of the (partly) oxidized Cu and Zn species in the catalyst surface. Earlier LEIS studies showed the validity of this approach, since copper oxide (27) and zinc oxide (28) show no matrix effects.

3.2. Dynamic Behavior

The surface atomic densities of ZnO and CuO have been determined with LEIS for ^{63}Cu/^{68}ZnO/SiO$_2$ reduced in pure H_2 at 473, 573, and 673 K. Figure 2 shows the CuO and ZnO percentages of the total surface area as a function of the applied 4-keV Ne^+ dose. As described above, a dose of 0.4×10^{15} ions/cm^2 corresponds to the removal of approximately one monolayer (ML). Hence, the data shown in Fig. 2 represent surface area percentages for depths of 0–7 ML.

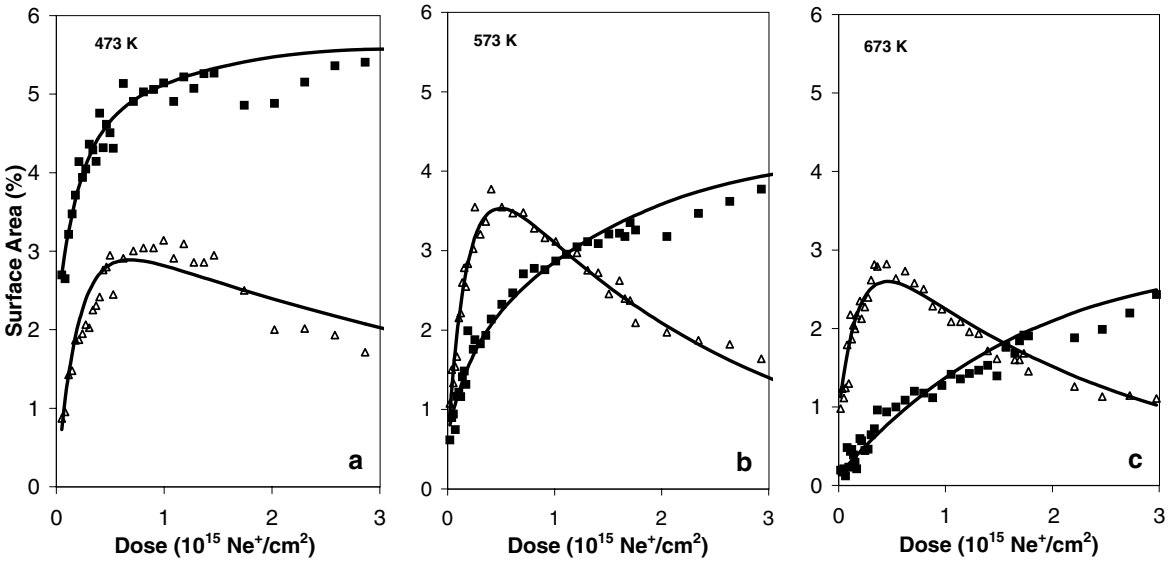

FIG. 2. The ZnO (open triangles) and CuO (solid squares) atomic densities as a function of a 4-keV Ne^+ dose for $Cu/ZnO/SiO_2$ after reduction in pure H_2 at 473 (a), 573 (b), and 673 K (c). All data were fitted using the same, constant values for the H, CuO, and ZnO sputter rates (solid lines).

Regardless of the applied reduction temperature, the data show a sharp increase in both the CuO and ZnO atomic densities for doses up to $\sim 0.25 \times 10^{15}$ ions/cm^2. This sharp increase may be explained by the presence of residual hydrogen (probably as hydroxyl groups) from the reductive treatment that remained on the surface after the evacuation treatment. Therefore, the depth profiles of the Cu (/Zn) LEIS yields were fitted by assuming the surface consisted of a combination of uncovered CuO and ZnO, as well as CuO and ZnO that were shielded either by hydrogen or by each other. All fits are based on the same, constant values for the sputter rates of H, CuO, and ZnO. The fits, represented by the solid lines in Fig. 2, show that hydrogen has a 13 times higher sputter yield than ZnO. This is in agreement with a reported 10–50 times higher sputter rate for hydrogen compared to that of other elements (29).

After the ZnO concentration at the surface increases, because of the hydrogen removal, it starts to decrease while the CuO surface concentration keeps increasing. Hence, the surface of $^{63}Cu/^{68}ZnO/SiO_2$ is enriched in ZnO following reduction. This is true even for reduction at 473 K; the extent of the enrichment in ZnO depends strongly on the reduction temperature. Figure 3 shows the surface composition (i.e., CuO and ZnO surface percentages deduced from fits for zero dose and in the absence of H) of $^{63}Cu/^{68}ZnO/SiO_2$ after reduction in H_2 at 473, 573, and 673 K. Note that the measurements before and after exposure to N_2O demonstrate that reduction at 473 K yields less than 4% of the Cu surface species in metallic form (see Section 3.1). Consequently, the surface concentration of metallic Cu after reduction at 473 K in pure H_2 is less than 0.2%. After reduction at 673 K, the surface concentration of metallic Cu is 3×10^2 ppm.

After reduction at 673 K about 96% of the cluster surface area is ZnO terminated and almost no CuO is exposed (see Fig. 3). This is in agreement with thermodynamics (19, 30). The low CuO content in the outermost layer also explains the absence of a sharply increasing CuO surface concentration as a function of dose on reduction at 673 K (see Fig. 2c). Following reduction at this temperature CuO is mainly covered with ZnO instead of hydrogen. In contrast, the fits show no significant shielding of ZnO by CuO, regardless of the applied reduction temperature.

Both Figs. 2 and 3 show a decrease in the total cluster area with increasing reduction temperatures. Reference (31) shows that such a decrease can be related to sintering. Hence, after reduction at 573 K and especially after reduction at 673 K, the clusters have partly sintered. TEM

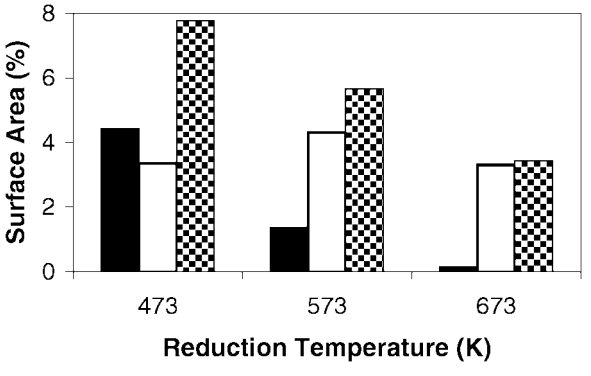

FIG. 3. The CuO (black bars), ZnO (white bars), and total CuO + ZnO (hatched bars) surface atomic densities as derived from the fits of the LEIS data after reduction in pure H_2. Note the decrease in the total cluster surface area because of sintering.

results confirm this: a combination of small (∼3 nm) and large (∼10 nm) clusters is observed on a catalyst reduced at 673 K, whereas a catalyst reduced at 473 K exposes only small clusters (∼3 nm).

Following reduction at 673 K the clusters have (partly) sintered and the overall amount of ZnO is high enough to cover the entire cluster surface. The LEIS measurements show that indeed 96% of the cluster surface area is covered with Zn species after reduction at 673 K. When in thermodynamic equilibrium, the ZnO enrichment is expected to be even higher for a reduction temperature of 473 K compared to that at a reduction temperature of 673 K. However, the complete amount of ZnO in the catalyst can cover at most 55% of the cluster surface area if the metal is spread over 3-nm clusters. After our 15-min reduction treatment only 44% of the cluster surface area was covered with Zn species. Hence, the concentration is kinetically determined. After prolonged exposure to H_2 at 473 K a cluster surface concentration of ∼55% may be expected.

During methanol synthesis, Cu/ZnO catalysts are not exposed to pure hydrogen but to CO/(CO_2)/H_2 mixtures. To study the effect of a methanol synthesis gas, we also analyzed a $^{63}Cu/^{68}ZnO/SiO_2$ catalyst pretreated in 5% CO/5% CO_2/90% H_2, a gas mixture that was also used by Grunwaldt *et al.* from Haldor Topsøe (12) to mimic industrially applied synthesis gas mixtures. In Fig. 4 the CuO and ZnO percentages of the total surface area are presented as a function of Ne^+ dose following treatments in 5% CO/5% CO_2/90% H_2 (solid data points) and in pure hydrogen (open data points) at 573 K. Following reduction in 5% CO/5% CO_2/90% H_2 the CuO (squares) and ZnO (triangles) surface areas are 11% lower than the corresponding signals after reduction in pure H_2. Exposure to N_2O following reduction in H_2 leads to a drop in the CuO and ZnO LEIS yields of less than 4% (after reduction at 473 K) and 20% (after reduction at 673 K) and we assume that the difference of 11% (reduction in 5% CO/5% CO_2/90% H_2 vs pure H_2 at 573 K) is likely caused by removal of the oxygen vacancies in the catalyst surface by CO_2 (32). Except for this difference, the treatments in 5% CO/5% CO_2/90% H_2 and pure H_2 produce very similar surfaces. In both cases one observes a surface that is enriched in ZnO, and the ZnO/Cu ratio upon low ion doses (reflecting the surface conditions) is much higher than the bulk value. From the measurements it may be concluded that a pretreatment in pure hydrogen leads to a slightly higher ZnO enrichment than does pretreatment in 5% CO/5% CO_2/90% H_2. However, the difference is small with respect to the earlier discussed temperature effect.

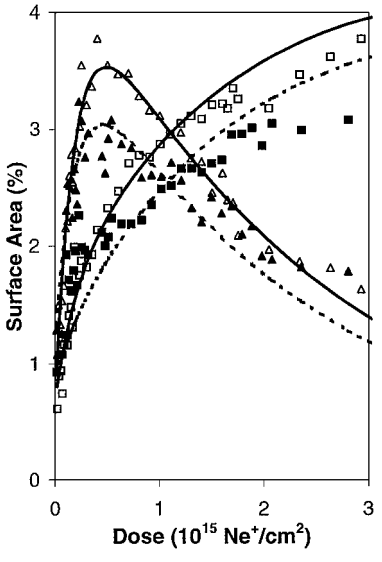

FIG. 4. The ZnO (triangles) and CuO (squares) atomic densities as a function of a 4-keV Ne^+ dose for Cu/ZnO/SiO_2. The open data points were obtained after reduction at 573 K in pure H_2; and the solid data points after reduction in 5% CO/5%CO_2/90% H_2. All data have been fitted (solid and dashed lines) using the same, constant values for the H, CuO, and ZnO sputter rates.

4. SURFACE STRUCTURE MODELS

Recently, Poels and Brands reviewed literature, catalytic tests, XRD, FT-IR, and preliminary LEIS analyses of the Cu/ZnO/SiO_2 catalyst (13). The results relevant for this paper are summarized here. Table 1 gives an overview of the results of catalyst activity tests concerning acetone hydrogenation, ester hydrogenolysis, and methanol synthesis (13). By way of comparison, the activity of unpromoted Cu/SiO_2 and Cu/MnO_x/SiO_2 are shown as well. Unpromoted Cu/SiO_2 has a modest activity, which essentially remains constant for all reactions as the reduction temperature is increased from 573 to 673 K. In contrast, Cu/ZnO/SiO_2 catalysts demonstrate a remarkable activity increase for higher catalyst reduction temperatures. Therefore, Poels and Brands proposed that the Cu–ZnO interface plays a crucial role in catalyzing these reactions. After reviewing literature and experimental evidence they reported two possible models that explain the enlarged interface after high-temperature reduction. The two models suggest either (i) migration of partly reduced ZnO on top of Cu or (ii) reversible formation of flat epitaxial Cu particles upon high-temperature reduction.

Three arguments would speak against model (i). For one, treatment in pure N_2 for 2 h of the reduced catalyst at a reduction temperature of 673 K partly reverses the observed increase in activity upon reduction. The reversibility of this was demonstrated by a subsequent repeated second reduction in H_2 at 673 K, resulting in exactly the same activity as was observed for a single reduction in hydrogen. This reversibility was considered inconsistent with alloy formation as the promoting effect. However, parts-per-million levels of O_2 due to leakage or other contaminants in the

TABLE 1

Summary of the Activity Data of Relevant Cu-Based Catalysts, with Reduction Temperatures of 573 and 673 K (13)

	Cu/SiO_2	$Cu/ZnO/SiO_2$	$Cu/MnO_x/SiO_2$
Methyl acetate hydrogenolysis, 573 K (673 K)	10% (10%)	20% (48%)	20% (27%)
Methyl palmitate hydrogenolysis, 573 K (673 K)	18% (18%)	40% (66%)	48% (52%)
Methanol synthesis, $CO/H_2 = 1/2$, 573 K ($CO/H_2 = 1/2$, 673 K)	0 nmol s^{-1} g^{-1} cat (0 nmol s^{-1} g^{-1} cat)	0 nmol s^{-1} g^{-1} cat (45 nmol s^{-1} g^{-1} cat)	—
Methanol synthesis, $CO/H_2 = 1/3$, 573 K ($CO/H_2 = 1/3$, 673 K)	5 nmol s^{-1} g^{-1} cat (8 nmol s^{-1} g^{-1} cat)	20 nmol s^{-1} g^{-1} cat 50 nmol s^{-1} g^{-1} cat	—

N_2 feed may well explain the observed deactivation during the 2-h inert treatment. Similarly to N_2O decomposition, trace amounts of O_2 may act to passivate the catalyst. Such a passivation, however, can be completely reversed by subsequent reduction without any loss of activity (33). The observed catalytic activity may be explained as follows: during either the "inert" or N_2O treatment the catalyst gets deactivated due to partial oxidation, and during the subsequent reduction Cu(I)/ZnO with oxygen vacancies is formed again and the catalyst is regenerated.

A second argument against model (i) concerns the reported similarity between activity as a function of reduction temperature of $Cu/ZnO/SiO_2$ and $Cu/MnO_x/SiO_2$ catalysts (13). It should be noted, however, that the increase in activity of the $Cu/ZnO/SiO_2$ is much more profound than that of the $Cu/MnO_x/SiO_2$ (Table 1).

A third argument against model (i) is formed by the absence of a peak shift in XRD that would accompany alloy formation (13). However, it should be noted that XRD is a bulk technique that selectively detects crystalline phases. Hence, amorphous or surface phases accompanying segregation, as shown by the LEIS measurements, would not be detected by this technique. Note that also EXAFS and even XPS may similarly average out segregation because of the probing depths of these techniques (34). In conclusion, there remain no serious arguments against model (i).

The present LEIS measurements confirm and extend earlier preliminary LEIS data, demonstrating that the surface of the $Cu/ZnO/SiO_2$ catalyst is strongly enriched in ZnO upon reduction, in agreement with model (i). The ZnO : CuO ratio increases by a factor of 7 when the reduction temperature is increased from 573 to 673 K. Moreover, there are strong indications for the presence of oxygen vacancies following reduction at 573 and 673 K, whereas these are completely absent after reduction at 473 K. This may well explain the fact that the methanol synthesis activity of the $Cu/ZnO/SiO_2$ catalyst in 33% CO_2/66% H_2 and 25% CO/75% H_2 mixtures increases from 0 nmol s^{-1} g^{-1} cat (at 573 K) to 45 nmol s^{-1} g^{-1} cat (673 K) and from 20 nmol s^{-1} g^{-1} cat (573 K) to 50 nmol s^{-1} g^{-1} cat (673 K), respectively.

Model (ii), the so-called Yurieva model, involves the reversible formation of flat epitaxial Cu particles upon high-temperature reduction from the fraction of the Cu dissolved in the mixed catalyst precursor phase. Using XRD and transmission electron microscopy (TEM), Yurieva *et al.* (35) observed the formation of flat epitaxial Cu particles on top of a Cu–Zn mixed oxide phase after a treatment under flowing hydrogen at 533 K. Formation of these epitaxial Cu particles correlated with enhanced hydrogenation activity. These authors showed that a maximum methanol formation rate is obtained for a catalyst containing about equal molar amounts of Cu and ZnO. In their study, the XRD and TEM analyses were performed on surfaces of Cu/ZnO and $Cu/ZnO/Al_2O_3$ catalysts with very low Cu : ZnO molar ratios (8% : 92% and 15% : 75%, respectively). Hence, one may question to what extent the active phase is present on the barely active catalyst that was investigated by Yurieva *et al.* The strongest argument in favor of the Yurieva model is the agreement between their model and the adsorptive N_2O decomposition data indicating an increasing Cu area after reduction. However, Berndt *et al.* (18) have clearly proven that in the case of reduced Cu/ZnO-based systems, this technique may very well produce misleading results. Our present results confirm this. While the weight increase upon N_2O chemisorption indicates a higher Cu^0 surface area upon reduction, the LEIS data suggest the reverse. Following reduction the catalyst surface is strongly enriched in ZnO. Moreover, combined N_2O chemisorption and LEIS data show that the oxidation behavior of the Cu in the catalyst is clearly different from that of pure metallic Cu. According to our measurements metallic Cu covers only 3×10^2 ppm of the $Cu/ZnO/SiO_2$ surface area (i.e., less than 1% of the cluster surface area) after reduction in H_2 at 673 K. Hence, the contribution of metallic Cu (platelets) is very limited at the surface of the most active catalyst. As indicated in Refs. (13, 19) the formation of epitaxial Cu platelets is also highly improbable from a thermodynamic point of view, since the surface free energy of Cu is much higher than that of ZnO (30).

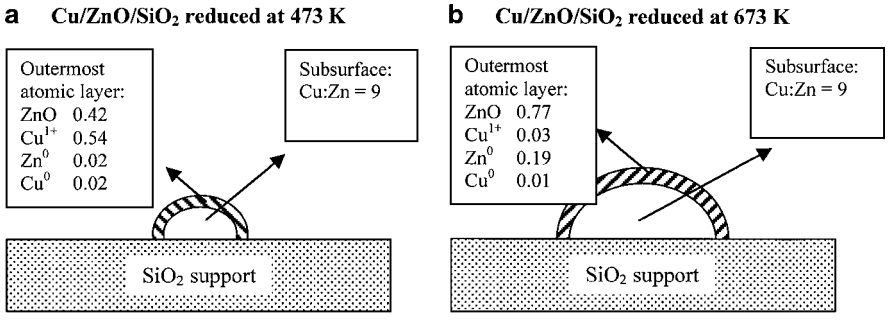

FIG. 5. Model of the surface structure of Cu/ZnO/SiO$_2$ after (a) low-temperature (473 K) and (b) high-temperature (673 K) reduction as determined with LEIS. One should note that the cluster shape represents an educated guess; it was not determined.

In conclusion, model (i), the migration of ZnO on top of Cu followed by the formation of a (partly) oxidized Cu in a Cu(I)/ZnO surface with oxygen vacancies present, seems the best hypothesis for formation of active sites of the Cu/ZnO/SiO$_2$ catalyst. Since the solubility of CuO in ZnO is limited (4–6% (w/w)), the Cu will be largely present as Cu^{1+} (5). Below the (partly) oxidized surface Cu^0 may well be present, as schematically indicated in Fig. 5, which shows a model of the surface structure derived from all measurements. For comparison low-temperature (473 K) and high-temperature (673 K) reduced catalysts are shown (Figs. 5a and 5b, respectively). As discussed in Section 3.2 the ZnO surface concentration is still kinetically determined after our reduction at 473 K. Prolonged reduction at this temperature would lead to complete ZnO segregation and cause a ZnO cluster surface concentration of ~55%. The observed weight increase in adsorptive N_2O decomposition could then be explained by the oxidation of the subsurface Cu atoms and the oxygen vacancies in the surface. According to (17, 36) the adsorptive N_2O decomposition method is not necessarily surface sensitive; the oxidation of subsurface Cu by N_2O is thus very well possible. Termination of Cu metal atoms by a (partly) oxidized overlayer is also favored by thermodynamics (19, 30). The valence states of the subsurface Cu and Zn are not known. However, only the presence of subsurface Cu in the metallic state can explain the results obtained with adsorptive N_2O decomposition. The maximum solubility of Cu in ZnO is 2% (37). Assuming that also the solubility of ZnO in Cu is small, the presence of subsurface metallic Cu would require reduction of most of the subsurface Zn species as well. Hence, the present model explains the catalytic tests and is in agreement with thermodynamics, adsorptive N_2O decomposition, LEIS measurements, and quasi *in situ* TEM measurements (38).

5. CONCLUSIONS

Both the catalytic activity and the surface composition of a $^{63}Cu/^{68}ZnO/SiO_2$ catalyst depend strongly on the applied reduction temperature in the range 473–673 K. LEIS data show that the catalyst surface is enriched in ZnO following reduction at 473 K. For reduction at 573 K the ZnO enrichment becomes more prominent and, finally, for reduction at 673 K virtually all Cu species in the catalyst surface are covered with ZnO. The ZnO surface enrichment of the $^{63}Cu/^{68}ZnO/SiO_2$ catalyst appears relatively insensitive to the reducing agent (being either $CO/CO_2/H_2$ or pure H_2).

The oxidation state of surface Cu species is obtained on the basis of the difference in the LEIS yields between metallic Cu and Cu oxide. By combining N_2O decomposition and LEIS it is demonstrated that the Cu LEIS yield of a reduced $^{63}Cu/^{68}ZnO/SiO_2$ catalyst decreases by less than 4% (after reduction at 473 K) and by 20% (after reduction 673 K) upon a N_2O decomposition treatment at 363 K. The Cu LEIS yield of a metallic ^{63}Cu reference sample decreases by a factor of 5! Moreover, the Zn yield decreases also by less than 4 and 20% after reduction at 473 and 673 K, respectively, suggesting a similar metal shielding by the oxygen atoms. Hence, the oxidation behavior of Cu at the Cu/ZnO/SiO$_2$ surface is clearly different from that of pure metallic Cu. This shows that the adsorptive decomposition of N_2O is not a straightforward manner for determining the Cu^0 surface area of reduced Cu/ZnO catalysts. However, the combined use of LEIS and adsorptive N_2O decomposition allows for a controlled and separate determination of the oxidation states of the Cu and Zn species in the outermost atomic layer of the catalyst surface.

The present results clearly show that ZnO segregates after reduction. The observed oxidation behavior of the Cu in the reduced Cu/ZnO/SiO$_2$ can only be explained in terms of the formation of Cu(I)/ZnO, along with oxygen vacancies. Since the methanol synthesis activity increases dramatically after reduction, these results strongly support theories (5, 6, 9, 11, 14–16) suggesting that Cu^{1+} is the active phase. Oxygen vacancies may also explain the fact that both the CuO and ZnO LEIS yields are ~11% lower after reduction at 573 K in 5% CO/5% CO_2/90% H_2 compared to reduction at 573 K in pure H_2.

It should be noted that our measurements leave hardly any room for the presence of metallic Cu at the surface. After reduction at 673 K (resulting in the highest activity in the methanol synthesis being 50 nmol s^{-1} g^{-1} cat for our

Cu/ZnO/SiO_2 catalyst) the metallic Cu surface concentration is 3×10^2 ppm (i.e., less than 1% of the cluster surface area).

ACKNOWLEDGMENTS

The authors gratefully acknowledge E. Timmermans and R. Rumphorst for their help in improving the energy resolution of the ERISS analyzer to enable separate detection of ^{63}Cu and ^{68}Zn. Dr. P. J. Kooyman of the National Centre for High-Resolution Electron Microscopy (Delft, The Netherlands) is gratefully acknowledged for performing the electron microscopy investigations. The Netherlands Organization for Scientific Research (NWO) is gratefully acknowledged for financial support.

REFERENCES

1. "American Methanol Institute," http:\\www.methanol.org.
2. Waugh, K. C., *Catal. Today* **15**, 51 (1992).
3. Yurieva, T., Plyasova, L. M., Makarova, O. V., and Krieger, T. A., *J. Mol. Catal. A* **113**, 455 (1996).
4. Yurieva, T., *Catal. Today* **51**, 457 (1999).
5. Klier, K., *Adv. Catal.* **31**, 243 (1982).
6. Ponec, V., *Surf. Sci.* **272**, 111 (1992).
7. Fujitani, T., and Nakamura, J., *Appl. Catal. A* **191**, 111 (2000).
8. Nakamura, J., Nakamura, I., Uchijima, T., Kanai, Y., Watanabe, T., Saito, M., and Fujitani, T., *J. Catal.* **160**, 25 (1996).
9. Spencer, M. S., *Top. Catal.* **8**, 259 (1999).
10. Topsøe, N.-Y., and Topsøe, H., *Top. Catal.* **8**, 267 (1999).
11. Fujitani, T., Nakamura, I., Uchijima, T., and Nakamura, J., *Surf. Sci.* **383**, 285 (1997).
12. Grunwaldt, J.-D., Molenbroek, A. M., Topsøe, N.-Y., Topsøe, H., and Clausen, B. S., *J. Catal.* **194**, 452 (2000).
13. Poels, E. K., and Brands, D. S., *Appl. Catal. A* **191**, 83 (2000).
14. Spencer, M. S., *Surf. Sci.* **192**, 323 (1987).
15. Spencer, M. S., *Surf. Sci.* **192**, 329 (1987).
16. Spencer, M. S., *Surf. Sci.* **192**, 336 (1987).
17. Skrzypek, J., Slozyński, J., and Ledakowicz, S., *in* "Methanol Synthesis, Science and Engineering," p. 45. Polish Scientific, Warsaw, 1994.
18. Berndt, H., Briehn, V., and Evert, S., *Appl. Catal. A* **86**, 65 (1992).
19. Viitanen, M. M., Janesn, W. P. A., Van Welzenis, R. G., and Brongersma, H. H., *J. Phys. Chem. B* **103**, 6025 (1999).
20. Brands, D. S., Poels, E. K., Krieger, T. A., Makarova, O. V., Weber, C., Veer, S., and Bliek, A., *Catal. Lett.* **36**, 175 (1996).
21. Brands, D. S., Poels, E. K., and Bliek, A., *Stud. Surf. Sci. Catal.* **101**, 1085 (1996).
22. Hellings, G. J. A., Ottevanger, H., Knibbeler, C. L. C. M., Van Engelshoven, J., and Brongersma, H. H., *Surf. Sci.* **162**, 913 (1985).
23. Bergmans, R. H., Kruseman, A. C., Severijns, C. A., and Brongersma, H. H., *Appl. Surf. Sci.* **70/71**, 283 (1993).
24. Matsunami, N., Yamamurra, Y., Itikawa, Y., Itoh, N., Kazumata, Y., Miyagawa, S., Morita, K., Shimizu, R., and Tawara, H., *Atom. Data Nucl. Data Tables* **31**, 1 (1984).
25. Evans, J. W., Wainwright, M. S., Bridgewater, A. J., and Young, D. J., *Appl. Catal.* **7**, 75 (1983).
26. Ovesen, C. V., Clausen, B. S., Schiøtz, J., Stoltze, P., Topsøe, H., and Nørskov, J. K., *J. Catal.* **168**, 133 (1997).
27. Mikhailov, S. N., Elfrink, R. J. M., Jacobs, J.-P., Oetelaar, L. C. A. Van de, Scanlon, P. J., and Brongersma, H. H., *Nucl. Instrum. Methods* **93**, 145 (1994).
28. Leerdam, G. C. Van, and Brongersma, H. H., *Surf. Sci.* **254**, 153 (1991).
29. Brongersma, H. H., Groenen, P. A. C., and Jacobs, J.-P., *in* "Science of Ceramic Interfaces II, 81 Materials Science Monographs" (J. Nowotny, Ed.), p. 113. Elsevier, Amsterdam/New York, 1994.
30. Overbury, S. H., Bertrand, P. A., and Somorjai, G. A., *Chem. Rev.* **75**(5), 547 (1975).
31. Jansen, W. P. A., Harmsen, J. M. A., Denier van der Gon, A. W., Hoebink, J. H. B. J., and Brongersma, H. H., *J. Catal.* **204**, 420 (2001).
32. Chinchen, G. C., Spencer, M. S., Waugh, K. C., and Whan, D. A., *J. Chem. Soc. Faraday Trans. 1* **83**, 2193 (1987).
33. Van den Scheur, F. Th, Brands, D. S., Van den Linden, B., Oude Luttikhuis, C., Poels, E. K., and Staal, L. H., *Appl. Catal. A* **116**, 237 (1994).
34. Jansen, W. P. A., Ruitenbeek, M., Denier van der Gon, A. W., Geus, J. W., and Brongersma, H. H., *J. Catal.* **196**, 379 (2000).
35. Yurieva, T. M., Plyasova, L. M., Kriger, T. A., Zaikovskii, V. I., Makarova, O. V., and Minyukova, T. P., *React. Kinet. Catal. Lett.* **51**, 495 (1993).
36. Luys, M. J., Van Oefelt, P. H., Brouwer, W. G. J., Pijpers, A. P., and Scholten, J. F. F., *Appl. Catal.* **46**, 161 (1989).
37. Klenov, D. O., Kryokova, G. N., and Plyasova, L. M., *J. Mater. Chem.* **8**, 1665 (1998).
38. Castricum, H. L., Ph.D. thesis. Amsterdam University, 2001.